EurJIC
European Journal of Inorganic Chemistry

Research Article
doi.org/10.1002/ejic.202400213

Chemistry Europe
European Chemical Societies Publishing

www.eurjic.org

Oligomer and Polymer: Self Assembly of [Cp*Fe(η^5-P_5)] and Ag(I) Salts of Bulky Weakly Coordinating Anions

Bijan Mondal,[a] Christoph Riesinger,[a] Martin Fleischmann,[a] and Manfred Scheer*[a]

Dedicated to Professor T. Fässler on the occasion of his 65th birthday

Reactions between the five-fold symmetric building block [Cp*Fe(η^5-P_5)] (**A**) and Ag(I) salts containing bulky weakly coordinating anions [TEF] and [FAL] ([TEF] = [Al{OC(CF_3)$_3$}$_4$]$^-$, [FAl] = [FAl{$OC_6F_{10}(C_6F_5)$}$_3$]$^-$) are presented. While, in the presence of Ag[TEF], **A** leads to the formation of a hitherto condensed 1D coordination polymer [{Ag(η^2:η^1-**A**)$_2$}]$_n$[TEF]$_n$ (**1**), a new finite tetranuclear Ag(I) complex [{Ag_4(η^1-**A**)$_2$(η^2:η^1-**A**)$_4$(η^1:η^1-**A**)$_2$}][FAL]$_4$ (**3**) was obtained with an Ag(I) salt bearing the weakly coordinating anion [FAl] increased in size. Various coordination modes (η^2:η^1; η^1:η^1 and η^1) of **A** were observed in the solid-state structure of **3**, reflecting the adaptive coordination behavior of **A** towards Ag(I) ions. Structural modifications of the 1D polymer (**1**) can be controlled by the addition of a limited amount of MeCN yielding the unwound heteroleptic 1D polymer [{Ag(MeCN)$_2$}$_3$(η^1:η^1:η^1-**A**)$_2$]$_n$[TEF]$_{3n}$ (**2**). Moreover, in the presence of MeCN, the finite oligomeric compound **3** can also be converted into a new heteroleptic 1D polymer [{Ag(MeCN)}$_4$(η^1:η^1-**A**)$_5$(η^2:η^1-**A**)$_2$]$_n$[FAL]$_{4n}$ (**4**). The solid-state structure of **4** discloses the existence of a unique 1,1,2-η^2:η^1 (π,σ) coordination of **A** along with 1,3-η^1:η^1 (σ) and 1,2-η^1:η^1 (σ) coordination modes, while 1,2,4-η^1:η^1:η^1 (σ) coordination modes of **A** were found in **2**. As revealed by X-ray crystallography, in all the cases, the cationic moieties are well separated from the weakly coordinating anions in the solid state.

Introduction

Coordination-driven self-assembly has shown its potential in designing fascinating molecular architectures connecting discrete building blocks through weak metal-ligand bonds.[1] Within this field, coordination polymers are of interest with regard to their physical, electronic, catalytic, and structural properties.[2] Such polymeric materials with the desired structure and functionality can be elegantly produced by sophisticated ligand desig and a targeted selection of metal ions.[3] The presence of anions also has also a great influence on the solid-state structure of the resulting compounds. Amongst the simplest are the one-dimensional (1D) coordination polymers featuring structures as for instance linear, zigzag, ladder, ribbon, helical, etc.[4] The most common strategy in this area exploits N-donor-containing organic ligands and heterocycles to connect different metal centers.[5] While organic molecules are widely utilized as linkers, the use of organometallic building blocks as connectors is occasional.[6]

Our research group successfully developed the concept of employing organometallic complexes containing polyphosphorus (P_n) ligands as connectors between metal ions.[7] In the presence of Cu(I) halides, the flexible coordination ability of the P_n ligand complexes enriches the library of neutral supramolecular aggregates comprising a wide spectrum of compounds spanning varieties from coordination polymers (1D, 2D and 3D) to nano-sized spheres, bowls, and capsules.[8] On the contrary, dimeric and polymeric as well as metal-deficient cage-like cationic compounds are obtained when Cu(I) and Ag(I) salts of weakly coordinating anions (WCA) are employed. In the presence of salts containing WCAs, P_n ligand complexes often exhibit dynamic processes in solution resulting in thermodynamically most stable products.

Regarding our efforts to study the remarkable coordination chemistry of naked P_n ligand complexes, we successfully employed the five-fold symmetric building block, [Cp*Fe(η^5-P_5)] (**A**).[10,11] **A** represents an impressive example of the diagonal relationship between carbon and phosphorus and can hence be correlated to the classical organometallic compound ferrocene.[12] The reaction of **A** with CuBr or CuI led to the quantitative formation of neutral 2D polymers [CuX(η^1:η^1:η^1-**A**)]$_n$ (X = Br, I).[13] However, in the presence of CuCl, a linear 1D polymer [CuCl(η^1:η^1-**A**)]$_n$[13] as well as an inorganic fullerene-like molecule [{(η^1:η^1:η^1:η^1:η^1-**A**)}$_{12}${CuCl}$_{10}${Cu_2Cl_3}$_5${Cu(CH_3CN)$_2$}$_5$] were obtained.[8b] New types of neutral organometallic-organic hybrid compounds were prepared by combining **A** with CuCl in the presence of pyridine-based organic linkers in three-component reactions.[14] Note that neutral self-assembled product formations are based on the presence of halide anions (Cl, Br and I) which are directly bonded to the Cu(I) ion. However, reacting **A** with the soft Lewis acidic Ag(I) bearing the bulky aluminate-

[a] Dr. B. Mondal, Dr. C. Riesinger, Dr. M. Fleischmann, Prof. Dr. M. Scheer
Institute of Inorganic Chemistry, University of Regensburg
93040 Regensburg (Germany)
E-mail: manfred.scheer@chemie.uni-regensburg.de

Supporting information for this article is available on the WWW under https://doi.org/10.1002/ejic.202400213

Research Article
doi.org/10.1002/ejic.202400213

Chemistry Europe
European Chemical Societies Publishing

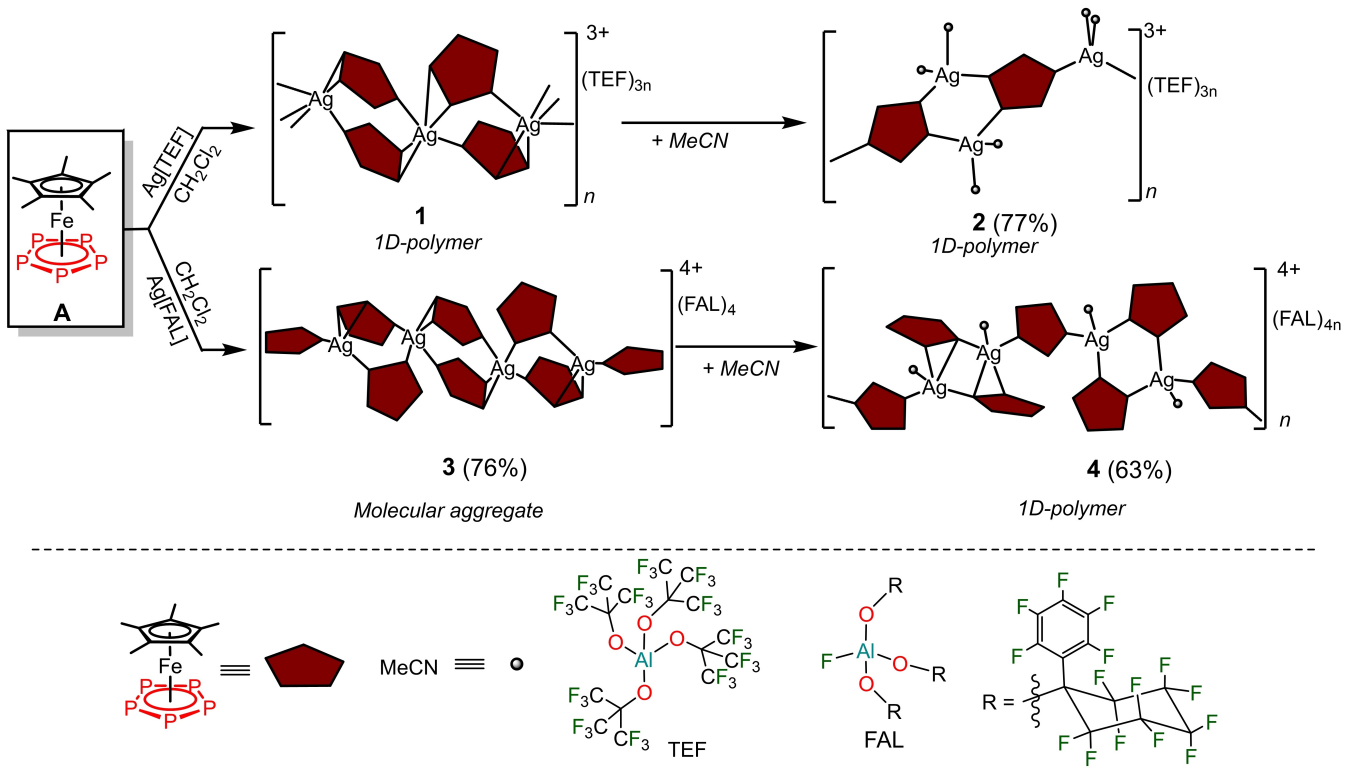

Scheme 1. Synthesis of the 1D polymer (**2**), molecular aggregate (**3**) and 1D-polymer (**4**) from **A** and Ag(I) WCA salts (WCA = TEF or FAL). Isolated yields are given in the parentheses.

based anion [TEF] (TEF = $[Al\{OC(CF_3)_3\}_4]^-$) which provides pseudo-gas phase conditions to Ag(I), the condensed 1D polymer $[Ag\{(\eta^2{:}\eta^1\text{-}\mathbf{A})\}_2]_n[TEF]_n$ (**1**) is formed.[10] It was observed that, in the solid state, the [TEF] anion provides better crystal packing to stabilize the 1D polymer, but **1** dissolves in solution (in CH_2Cl_2) by depolymerization to a mono-cation which exists in dynamic equilibria with the polycationic species. It is worth noting that polymeric assemblies of spherical cages were reported not long since.[15a] Thus, the question arose whether the size of the bulky WCAs has an influence on the structural outcome. Therefore, Ag[FAL] ([FAl] = $[FAl\{OC_6F_{10}(C_6F_5)\}_3]^-$)[15b] was chosen to react with **A** (Scheme 1). Furthermore, the influence of the limited amount of coordinating MeCN, which serves as a model CN-containing reagent in the self-assembly of **A** with Ag[X] (X = TEF and FAL), has to be studied. Herein we present the syntheses, solid-state structures and spectroscopic characterizations of the finite tetranuclear oligomer $[\{Ag_4(\eta^1\text{-}\mathbf{A})_2(\eta^2{:}\eta^1\text{-}\mathbf{A})_4(\eta^1{:}\eta^1\text{-}\mathbf{A})_2\}][FAL]_4$ (**3**), in contrast to usually formed polymeric chain with TEF as counterion, as well as the MeCN incorporated fine-tuned heteroleptic infinite 1D polymer $[\{Ag(MeCN)_2\}_3(\eta^1{:}\eta^1{:}\eta^1\text{-}\mathbf{A})_2]_n[TEF]_{3n}$ (**2**) and the 1D polymer $[\{Ag(MeCN)\}_4(\eta^1{:}\eta^1\text{-}\mathbf{A})_5(\eta^2{:}\eta^1\text{-}\mathbf{A})_2]_n[FAL]_{4n}$ (**4**). Various coordination modes of **A** were observed in the solid-state structures of **2**–**4** revealing the adaptive coordination behavior of **A** towards Ag(I) ions. In addition, an enhanced solubility of **2**–**4** was observed owing to the influence of the bulky weakly coordinating anions.

Results and Discussion

Self-Assembly of A with Ag[FAL]: Tetranuclear Complex $[\{Ag_4(\eta^1\text{-}\mathbf{A})_2(\eta^2{:}\eta^1\text{-}\mathbf{A})_4(\eta^1{:}\eta^1\text{-}\mathbf{A})_2\}][FAL]_4$ (3)

Compound **3** was obtained when two equivalents of **A** were treated with Ag[FAL] in CH_2Cl_2 and stirred at room temperature. After 3 h of stirring, the initial green color of **A** had changed to brown. Upon layering the crude mixture with *n*-pentane, red crystalline plates of $[\{Ag_4(\eta^1\text{-}\mathbf{A})_2(\eta^2{:}\eta^1\text{-}\mathbf{A})_4(\eta^1{:}\eta^1\text{-}\mathbf{A})_2\}][FAL]_4$ (**3**) suitable for single-crystal X-ray structure analysis were isolated.

Compound **3** crystallizes in the monoclinic space group $P2_1/n$ (Table 1). The solid-state structure (Figure 1) reveals the formation of a finite tetranuclear molecular aggregate $[Ag_4(\mathbf{A})_8]^{4+}$. In contrast, the formation of the 1D polymer **1** was observed when **A** was reacted with Ag[TEF] under similar reaction conditions.[1] This change in the structural outcome can be attributed to the enhanced size of the WCA from [TEF] (57 atoms, 12.5 Å) to [FAl] (86 atoms, 14.9 Å) which obviously triggers the formation of the tetranuclear complex **3**.[16] As the stability of the ionic structure is heavily influenced by the relative size and charge of the ions involved, the bulky size of the WCA is assumed to play an important role in forming the tetranuclear complex **3** in the solid state. Taking a closer look at the X-ray structure, all molecules of **A** (**I**–**IV**, Figure 1) are identified to show different coordination modes. While **IV** is only end-on σ coordinating to one Ag atom, **III** is bridging two Ag atoms in a 1,2-$\eta^1{:}\eta^1$-(σ) coordination mode. A 1,2,3-$\eta^2{:}\eta^1$-(π,

Research Article
doi.org/10.1002/ejic.202400213

Table 1. Crystallographic data for compounds **2**–**4**.

	2	**3**	**4**
Formula	$C_{80}H_{48}Ag_3Al_3F_{108}Fe_2N_6O_{12}P_{10}$, 0.6[$C_2H_3N$]	$C_{112}H_{60}Ag_2Al_2F_{92}Fe_4O_6P_{20}$, [$CH_2Cl_2$]	$C_{106}H_{51}Ag_2Al_2F_{92}Fe_3N_2O_6P_{15}$, 1.75[$CH_2Cl_2$]
D_{calc}/g cm^{-3}	1.983	1.945	1.963
μ/mm^{-1}	8.040	8.976	8.422
Formula Weight	4187.80	4447.02	4246.91
Color	clear light orange	clear dark red	clear red
Shape	block-shaped	plate-shaped	block-shaped
Size/mm^3	0.30×0.23×0.12	0.12×0.10×0.05	0.31×0.17×0.14
T/K	123.00(10)	122.9(3)	100.01(10)
Crystal System	triclinic	monoclinic	monoclinic
Flack Parameter	–	–	0.0514(19)
Hooft Parameter	–	–	−0.0094(5)
Space Group	$P\bar{1}$	$P2_1/n$	$C2$
a/Å	18.0853(2)	23.46600(10)	35.13731(11)
b/Å	18.7408(2)	19.73020(10)	18.57647(5)
c/Å	22.8030(3)	34.5185(2)	22.11572(6)
α/°	96.2070(10)	90	90
β/°	91.2030(10)	108.1600(10)	95.4143(3)
γ/°	113.7680(10)	90	90
V/Å^3	7013.98(15)	15185.63(16)	14371.13(7)
Z	2	4	4
Z'	1	1	1
Wavelength/Å	1.54184	1.54184	1.54184
Radiation type	Cu K_α	Cu K_α	Cu K_α
Q_{min}/°	2.597	2.991	2.007
Q_{max}/°	68.249	66.656	74.997
Measured Refl.	105266	104872	140783
Independent Refl.	25542	26626	29072
Reflections with I > 2(I)	22244	16605	28684
R_{int}	0.0811	0.0565	0.0224
Parameters	3123	2282	2200
Restraints	3389	365	169
Largest Peak	1.708	0.679	1.047
Deepest Hole	−0.871	−0.709	−0.720
GooF	1.091	0.740	1.036
wR_2 (all data)	0.2229	0.0551	0.0653
wR_2	0.2179	0.0522	0.0652
R_1 (all data)	0.0818	0.0544	0.0247
R_1	0.0770	0.0293	0.0244

σ) coordination mode bridging two Ag atoms can be found in **II**, which was also experimentally observed in **1**. Finally, **I** shows a bridging 1,2,4-η^2:η^1-(π, σ) coordination mode. This results in two different types of coordination environments around the Ag(I) centers, with one of them connecting to three and the other one to four *cyclo*-P_5 moieties of **A** molecules. The lengths of the Ag–P bonds are strongly dependent on the bonding mode. While σ coordination results in Ag–P bond lengths of about 2.5 Å, π coordination results in Ag–P distances of about 2.7–2.8 Å. The P–P bond lengths of **3** are relatively uniform [2.1069(15)–2.1698(14) Å), which is in good agreement with the average P–P bond length of 2.1383(14) Å determined for the free complex **A**.[10] Only the π coordinating P–P bonds are slightly elongated with P3–P4 at 2.1704(14) Å and P7–P8 at 2.1539(14) Å. In the monoclinic crystal system of **3**, the $[Ag_4(\mathbf{A})_8]^{4+}$ aggregates are surrounded by the non-coordinating [FAL] anions, which separate the cationic fragments from each other (Figure S5).

The $^{31}P\{^1H\}$ NMR spectrum of **3** in solution shows a singlet at $\delta = 153.2$ ppm slightly shifted to lower field compared to the

Research Article
doi.org/10.1002/ejic.202400213

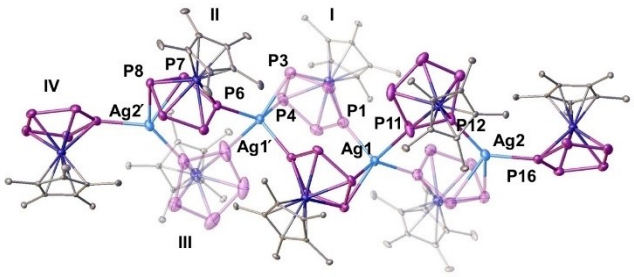

Figure 1. Solid-state structure of compound **3**. ADPs (anisotropic displacement parameters) are drawn at 50% probability. Anion and H atoms are omitted for clarity and C atoms are shown in smaller sizes. Selected bond lengths [Å]: P1–Ag1 2.5348(10), P3–Ag1' 2.6627(10), P4–Ag1' 2.7887(10), P6–Ag1' 2.4926(9), P7–Ag2' 2.8266(10), P8–Ag2' 2.8097(10), P11–Ag1 2.6100(11), P12–Ag2 2.4781(11), P16–Ag2 2.4719(10).

uncoordinated **A** ($\delta = 151$ ppm). In the positive mode electrospray ionization mass spectrometry (ESI-MS), a major peak at 798.8 corresponding to the mono cation $[Ag(\mathbf{A})_2]^+$ can be observed. This suggests a fast, dynamic behavior in solution, which is quite common when P_n ligand complexes coordinate to a flexible Ag(I) center containing a WCA. The ^1H and $^{19}F\{^1H\}$ NMR spectra show the characteristic signals for the Cp* ligand as well as the [FAl] anion. The latter was also confirmed by the negative mode ESI-MS.

1D Polymer $[\{Ag(MeCN)_2\}_3(\eta^1{:}\eta^1{:}\eta^1\text{-}A)_2]_n[TEF]_{3n}$ (2) and 2D Polymer $[\{Ag(MeCN)\}_4(\eta^1{:}\eta^1\text{-}A)_5(\eta^2{:}\eta^1\text{-}A)_2]_n[FAL]_{4n}$ (4)

The formation of supramolecular assemblies is susceptible to reaction conditions, hence the structural outcome depends on the stoichiometry, type and size of the anions as well as of the solvents. Subsequently, we employed the coordinating nature of MeCN, as a synthon of a CN-functional group containing a simple molecule, to achieve structural variety. Therefore, a limited amount (see the supporting information) of MeCN was added to the crude reaction mixtures of the synthesis of the 1D polymer **1** and the tetranuclear complex **3**, respectively, which resulted in orange and red crystals of **2** and **4** upon layering the crude reaction mixture with *n*-hexane. Note that the addition of an excess of MeCN produces soluble products which could not be isolated regardless of numerous attempts. The results demonstrated that adding a limited amount of MeCN allowed to isolate the polymeric assemblies **2** and **4** which showed a more relaxed coordination environment around the Ag(I) centers as compared to the starting materials. The Ag(I) centers were coordinated to one (**4**) or two (**2**) molecules of MeCN.

The molecular structure of **2** (Figure 2a) reveals a unique heteroleptic 1D polymer of the general formula $[\{Ag(MeCN)_2\}_3(\eta^1{:}\eta^1{:}\eta^1\text{-}A)_2]_n[TEF]_{3n}$. In Figure 2a, the linear 1D chain structure of **2** is depicted, which consists of virtually planar six-membered $\{Ag_2P_4\}$ rings (folding angle 0.43(10)°), which are bridged by additional $Ag(MeCN)_2$ moieties. Therefore, each *cyclo*-P_5 unit of **A** exhibits a 1,2,4-$\eta^1{:}\eta^1{:}\eta^1$ (σ) coordination mode. This results in tetrahedral arrangements for each Ag(I) ion coordinated to two units of **A** through a σ-η^1 mode and two MeCN ligands. The [Cp*Fe] fragments point to opposite sides of the $\{Ag_2P_4\}$ plane in such a way that the *cyclo*-P_5 planes become coplanar with the $\{Ag_2P_4\}$ planes (plane twist angle 179.71(5) °). The structure of **2** can be compared to the 1D polymeric structure $[CuCl(\eta^1{:}\eta^1\text{-}\mathbf{A})]_n$, with the difference that the $\{Ag_2P_4\}$ cycles in **2** are bridged via $Ag(MeCN)_2$ moieties, whereas the $\{Cu_2P_4\}$ cycles in $[CuCl(\eta^1{:}\eta^1\text{-}\mathbf{A})]_n$ are bridged by the Cl atoms (Figure S8).[12] The infinite heteroleptic 1D polymer **2** is essentially comparable to the infinite homoleptic chain of **1** as both are composed of **A** and Ag(I). However, **2** additionally incorporates MeCN ligands, which change the coordination environment around the Ag(I) ions. In the polycationic chain of **1**, each Ag(I) ion is doubly bridged by the *cyclo*-P_5 units of two molecules of **A** in the 1,2,3-$\eta^2{:}\eta^1$(mixed π,σ) coordination mode producing six-membered $\{Ag_2P_4\}$ and three-membered $\{AgP_2\}$ cycles. This results in an unusual tetrahedral coordination mode around Ag(I) which virtually connects to a total of six P atoms. On the other hand, the X-ray structure of **4** (Figure 2b) corresponds to a new heteroleptic 1D infinite chain comprising six-membered $\{Ag_2P_4\}$, four-membered $\{Ag_2P_2\}$ and three-membered $\{AgP_2\}$ cycles (Figure 2b). The butterfly-shaped $\{Ag_2P_2\}$ cycles (folding angle 34.82(6)°)[17] are fused to two $\{AgP_2\}$ triangles through two opposite Ag–P edges. This gives rise to two completely distinct Ag–P bond lengths of 2.896(13) and 2.533(10) Å. Both the Ag–P bond lengths are markedly different from those observed in **1** (2.590(2)–2.824(3) Å). The Ag–P bond lengths of **4** within the $\{Ag_2P_4\}$ rings (2.480(1) and 2.499(10) Å) are even shorter than those of **1**. The Ag–P bond lengths vary

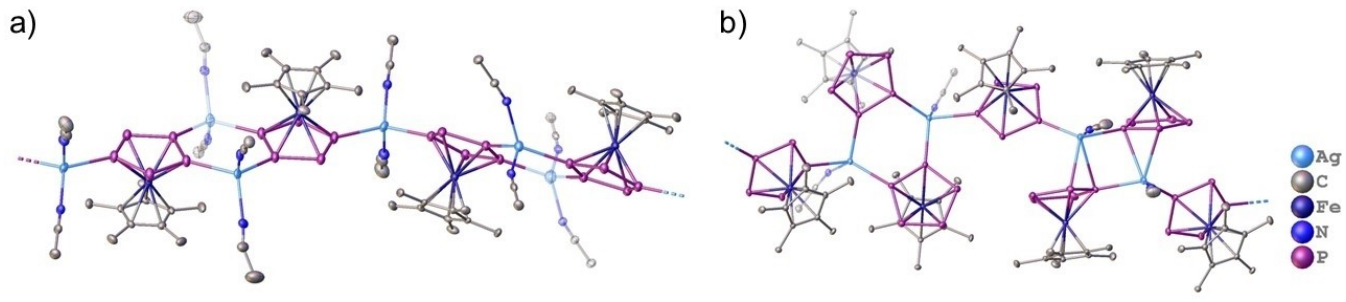

Figure 2. Section of (a) 1D polymer **2** and (b) 1D polymer **4** in the solid state. ADPs (anisotropic displacement parameters) are drawn at 50% probability. Anions and H atoms are omitted for clarity, C and N atoms are shown in smaller sizes for clarity.

Research Article
doi.org/10.1002/ejic.202400213

depending upon the type of coordination (σ or π). Usually, the π-coordination results in longer Ag–P bond lengths compared to the σ-coordination. On the contrary, uniform and relatively shorter Ag–P bond lengths are observed in **2** (2.460(6)–2.490(12) Å). Note that two [Cp*Fe] fragments in **4** are oriented along the same direction resulting in boat-shaped $\{Ag_2P_4\}$ rings (folding angle 27.02(3) °). The $\{Ag_2P_4\}$ and $\{Ag_2P_2\}$ rings are bridged by one unit of **A** through 1,3-η^1:η^1 (σ) coordination. Therefore, three noticeably different types of Ag–P coordination of the *cyclo*-P_5 units of **A** were observed: 1,2-η^1:η^1, 1,3-η^1:η^1 and 1,1,2-η^2:η^1 that result in two dissimilar environments around the Ag(I) ions. Apart from being coordinated to an MeCN ligand, the Ag(I) ions within the six-membered rings are connected to three η^1(σ)-coordinated *cyclo*-P_5 units of three **A** molecules, whereas the other Ag(I) centers are connected to one η^2(π)- and two η^1(σ)-coordinated *cyclo*-P_5 units of three **A** molecules. The observed P–P bond lengths in **2** (2.103(2)–2.111(18) Å) and **4** (2.101(11)–2.121(14) Å) are essentially consistent with those of the uncoordinated complex **A** as determined by X-ray diffraction (2.116(2)–2.127(2) Å) and by electron diffraction (2.117(4) Å).[18] A P–P bond length of 2.140(15) Å was found within the $\{AgP_2\}$ triangle of **4**. The Ag(I) ions form chains along the crystallographic *abc* plane in **2** and the crystallographic *c*-axis in **4** both of which are surrounded by coordinating moieties of **A** and MeCN ligands. These polycationic chains are separated from each other by bulky counterions (Figures S4 and S6).

Compounds **2** and **4** are readily soluble in CH_2Cl_2 but insoluble in alkanes. The $^{31}P\{^1H\}$ NMR spectrum of **2** in CD_2Cl_2 shows a singlet at $\delta = 150.1$ ppm which is slightly upfield shifted compared to that of **1** ($\delta = 154.2$), but comparable to that of uncoordinated **A**.[10] On the other hand, the $^{31}P\{^1H\}$ NMR spectrum of **4** shows signals similar to **3** (at $\delta = 153.8$ ppm). The ^1H NMR spectra of **2** and **4** in CD_2Cl_2 show signals related to the Cp* ligands around $\delta = 1.4$ ppm whereas signals corresponding to MeCN are located at $\delta = 2.50$ (for **2**) and 2.05 ppm (for **4**). The $^{13}C\{^1H\}$ NMR spectra also show signals corresponding to the Cp* and coordinated MeCN ligands. The $^{19}F\{^1H\}$ NMR spectrum of **4** reveals a characteristic set of signals related to the [FAl] anion while that of **2** displays a singlet at $\delta = -75.6$ ppm corresponding to the [TEF] anion. The existence of the [TEF] and [FAL] counter ions is confirmed by negative mode ESI-MS measurements. A common signal at $m/z = 798.7$ in the positive mode ESI-MS (from CH_2Cl_2 solutions) was observed both in **2** and **4** and can be assigned to the mono-cationic fragment $[Ag(\mathbf{A})_2]^+$. Additionally, **2** displays a peak at $m/z = 535.5$ corresponding to $[(\mathbf{A})Ag(MeCN)_2]^+$ while **4** displays the existence of the $[(\mathbf{A})Ag(MeCN)]^+$ fragment at $m/z = 493.8$.

Conclusions

In summary, we could show the impact of the size of the anion on the structural outcome of the self-assembly of [Cp*Fe(η^5-P_5)] (**A**) and Ag(I) salts. By using bulkier [FAL] instead of [TEF], we were able to isolate a finite tetranuclear complex $[\{Ag_4(\eta^1\text{-}\mathbf{A})_2(\eta^2\text{:}\eta^1\text{-}\mathbf{A})_4(\eta^1\text{:}\eta^1\text{-}\mathbf{A})_2\}][FAL]_4$ (**3**), instead of an infinite polymeric chain. Furthermore, MeCN was exploited as a model coordinating reagent containing a CN functional group in the self-assembly reaction. Therefore, the addition of MeCN partially replaces the *cyclo*-P_5 ligands of **A** and thereby changes the coordination environment of the Ag(I) centers resulting in the formation of infinite 1D ($[\{Ag(MeCN)_2\}_3(\eta^1\text{:}\eta^1\text{:}\eta^1\text{-}\mathbf{A})_2]_n[TEF]_{3n}$ (**2**)) and 1D ($[\{Ag(MeCN)\}_4(\eta^1\text{:}\eta^1\text{-}\mathbf{A})_5(\eta^2\text{:}\eta^1\text{-}\mathbf{A})_2]_n[FAL]_{4n}$ (**4**)) polymeric chains, the structures of which are much more relaxed compared to the starting materials. Although the compositions of **2** and **4** are essentially similar as both of them contain **A**, Ag(I) and labile MeCN ligands, the structural differences are based on the differently sized [TEF] and [FAL] anions. Moreover, the infinite chains **2** and **4** present promising building blocks for extended organometallic-organic hybrid networks by replacing the labile MeCN ligands with multitopic linkers. We are currently conducting further studies in this direction.

Experimental Section

General Information

All manipulations were carried out under an inert atmosphere of dry nitrogen using standard glove-box and Schlenk techniques. The nitrogen was dried and purified from traces of oxygen/water with a $Cu/MgSO_4$ catalyst, concentrated H_2SO_4 and orange gel. All used solvents were taken from the solvent purification system MB SPS-800 of the company MBRAUN. The precursors [Cp*FeP_5],[19] [Ag][TEF][20] and $[Ag(CH_2Cl_2)][FAL]$[15b] were prepared according to literature procedures. $[AgBF_4]$ was purchased from the company TCI and used without further purification. Solution NMR spectra were recorded on a Bruker Avance III HD 400 spectrometer (^1H: 400 MHz, ^{31}P: 161 MHz, ^{13}C: 100 MHz, ^{19}F: 376 MHz) with dichloromethane-d_2 as solvent at room temperature. The signals of tetramethylsilane (^1H, ^{13}C), $CFCl_3$ (^{19}F), and 85 % H_3PO_4 (^{31}P) were used as reference for determining chemical shifts. The chemical shifts δ are presented in parts per million ppm. The spectra were processed and analyzed using the software Bruker TopSpin 3.0. Elemental analyses were performed on an Elementar vario MICRO cube apparatus at the microanalytical laboratory of the University of Regensburg. Mass spectra (ESI-MS) were measured on a Finnignan Thermoquest TSQ 7000 mass spectrometer or Agilent Q-TOF 6540 UHD mass spectrometer.

Synthesis of $[\{Ag(MeCN)_2\}_3(\eta^1\text{:}\eta^1\text{:}\eta^1\text{-}\mathbf{A})_2]_n[TEF]_{3n}$ (2)

MeCN (0.5 ml) was added dropwise to *in-situ* prepared **1**, which was obtained by stirring **A** (14 mg, 0.04 mmol, 5 ml CH_2Cl_2) and Ag[TEF] (31 mg, 0.026 mmol, 5 ml CH_2Cl_2) at room temperature for 6 h. The resultant mixture was stirred for 1 h at room temperature. The mixture was filtered, layered with *n*-hexane and stored at RT to obtain orange blocks of **2**. The crystals were washed with hexane (3x5 ml) and dried under reduced pressure. Yield: 29 mg (0.0068 mmol, 77 % with respect to Ag[TEF]). ^1H NMR (CD_2Cl_2, 27 °C, 400 MHz, ppm): $\delta = 2.50$ (br, $\underline{Me}CN$), 1.42 (s; $C_5\underline{Me}_5$). $^{13}C\{^1H\}$ NMR (CD_2Cl_2, 27 °C, 100 MHz, ppm): $\delta = 123.3$ (Me$\underline{C}$N), 120.4 (Me$\underline{C}$N), 96.3 ($\underline{C}_5Me_5$), 15.1 ($\underline{Me}CN$), 11.3 ($C_5\underline{Me}_5$). $^{19}F\{^1H\}$ NMR (CD_2Cl_2, 27 °C, 376.5 MHz, ppm): $\delta = -75.59$ (s,TEF). $^{31}P\{^1H\}$ NMR (CD_2Cl_2, 27 °C, 161.98 MHz, ppm): $\delta = 150.14$ (s, [Cp*Fe$\underline{P}_5$]). Elemental analysis (%) calculated for $C_{80}H_{48}Ag_3Al_3F_{108}Fe_2N_6O_{12}P_{10}$: C, 23.08; H, 1.16; N, 2.02 found: C, 22.95; H, 1.05; N, 1.89. ESI-MS (CH_2Cl_2, RT, positive): $m/z = 798.7422$ $[(\mathbf{A})_2Ag]^+$, 535.5302 $[(\mathbf{A})Ag(MeCN)_2]^+$. ESI-MS ($CH_2Cl_2$, RT, negative): $m/z = 966.6293$ (TEF^-).

Research Article
doi.org/10.1002/ejic.202400213

Synthesis of [{Ag$_4$(η^1-A)$_2$(η^2:η^1-A)$_4$(η^1:η^1-A)$_2$}][FAL]$_4$ (3)

32 mg (0.02 mmol, 1 eq.) Ag(CH_2Cl_2)[FAl] and 14 mg (0.04 mmol, 2 eq.) [Cp*Fe(η^5-P_5)] (**A**) are each dissolved in 5 mL CH_2Cl_2 in separate Schlenk vessels. Upon addition of the Ag^+ solution to the stirred **A** solution, the initial dark green color turned to olive green and subsequently to light brown. After 3 h of stirring at room temperature, the solution was filtered and carefully layered with the fivefold volume of *n*-pentane. In the course of minutes, the formation of small amounts of crystalline product was observed at the mixing zone of CH_2Cl_2 and *n*-pentane. The layered system was stored at +4 °C and in the course of one-week compound **3** can be obtained as small red crystalline plates. The crystals are filtered off, washed with *n*-pentane (3×10 mL) and dried in vacuum. Yield: 34 mg (0.0076 mmol, 76 % with respect to Ag(CH_2Cl_2)[FAl]). ^{1}H NMR (CD_2Cl_2, 27 °C, 400 MHz, ppm): δ = 1.41 (s; $C_5\underline{Me}_5$). ^{13}C{^{1}H} NMR (CD_2Cl_2, 27 °C, 100 MHz, ppm): δ = 14.4 (s, $C_5\underline{Me}_5$), 106.1 (s, $\underline{C}_5Me_5$). ^{19}F{^{1}H} NMR (CD_2Cl_2, 27 °C, 376.5 MHz, ppm): δ = –112.3 (d, 2F), –116.8 (d, 2F), –121.6 (d, 2F), –127.8 (s, 2F), –130.4 (d, 2F), –136.9 (d, 2F), –140.7 (d, 1F), –154.3 (t, 1F), –164.6 (t, *J*F,F = 18 Hz, 1F), –171.8 ppm (s, AlF). ^{31}P{^{1}H} NMR (CD_2Cl_2, 27 °C, 161.98 MHz, ppm): δ = 153.24 (s, [Cp*Fe$\underline{P}_5$]). Elemental analysis (%) calculated for $C_{56}H_{30}Fe_2P_{10}F_{46}Al_4Ag$: C, 30.38; H, 1.37. Found: C, 30.74; H, 1.44. ESI-MS (CH_2Cl_2, RT, positive): *m/z* (%) = 798.8 [Ag{Cp*FeP_5}$_2$]$^+$ (95 %). ESI-MS (CH_2Cl_2, RT, negative): 1381.3 [FAL]$^-$.

Synthesis of [{Ag$_4$(η^1-A)$_2$(η^2:η^1-A)$_4$(η^1:η^1-A)$_2$}][FAL]$_4$ (3)

MeCN (0.5 ml) was added dropwise to *in-situ* prepared **3**, which was obtained by stirring **A** (14 mg, 0.04 mmol, 5 ml CH_2Cl_2) and Ag(CH_2Cl_2)[FAl] (32 mg, 0.02 mmol, 5 ml CH_2Cl_2) at room temperature for 2 h. The resultant mixture was stirred for 4 h at room temperature. The mixture was filtered, layered with *n*-hexane and stored at RT to obtain red blocks of **4**. The crystals were washed with hexane (3x5 ml) and dried under the reduced pressure. Yield: 27 mg (0.0063 mmol, 63 % with respect to Ag(CH_2Cl_2)[FAl]). ^{1}H NMR (CD_2Cl_2, 27 °C, 400 MHz, ppm): δ = 2.05 ($\underline{Me}$CN), 1.38 ($C_5\underline{Me}_5$). ^{13}C{^{1}H} NMR (CD_2Cl_2, 27 °C, 100 MHz, ppm): δ = 121.4 (Me$\underline{C}$N), 95.7 ($\underline{C}_5Me_5$), 13.8 ($\underline{Me}$CN), 11.2 ($C_5\underline{Me}_5$). ^{19}F{^{1}H} NMR (CD_2Cl_2, 27 °C, 376.5 MHz, ppm): δ = –112.32 (d, *J*F,F = 286 Hz, 2F), –116.79 (d, *J*F,F = 292 Hz, 2F), –121.59 (d, *J*F,F = 296 Hz, 2F), –127.92 (s, 2F), –130.32 (d, *J*F,F = 268 Hz, 2F), –136.94 (d, *J*F,F = 298 Hz, 2F), –141.04 (d, *J*F,F = 327 Hz, 1F), –154.40 (t, *J*F,F = 18 Hz, 1F), –165.05 (t, *J*F,F = 21 Hz, 1F), –171.89 ppm (s, AlF). ^{31}P{^{1}H} NMR (CD_2Cl_2, 27 °C, 161.98 MHz, ppm): δ = 153.83 (s, [Cp*Fe$\underline{P}_5$]). Elemental analysis (%) calculated for $C_{106}H_{51}Ag_2Al_2F_{92}Fe_3N_2O_6P_{15}$: C, 31.07; H, 1.25; N, 0.68. Found: C, 31.24; H, 1.30; N, 0.72. ESI-MS (CH_2Cl_2, RT, positive): *m/z* = 798.6633 [(**A**)$_2$Ag]$^+$, 493.8338 [(**A**)Ag(MeCN)]$^+$. ESI-MS (CH_2Cl_2, RT, negative): 1380.87 [FAL]$^-$.

Supporting Information

Experimental procedures for the synthesis of all compounds, analytical data and X-ray crystallographic details are summarized in the Supporting Information. Deposition Numbers CCDC-2343380 (**2**), CCDC-2343381 (**3**) and CCDC-2343382 (**4**) contain the supplementary crystallographic data for this paper. These data are provided free of charge by the joint Cambridge Crystallographic Data Centre and Fachinformationszentrum Karlsruhe Access Structures service. The authors have cited additional references within the Supporting Information.[21–27]

Acknowledgements

The Deutsche Forschungsgemeinschaft (DFG) is gratefully acknowledged for the support within the project Sche 384/42-1 and 44-1. B.M. is grateful to the Alexander von Humboldt Foundation for his postdoctoral fellowship. C. R. is grateful to the Studienstiftung des Deutschen Volkes for his PhD fellowship. Lukas Adlbert is acknowledged for recording the mass spectra. Dr. Michael Seidl is gratefully acknowledged for the initial help with the X-ray measurements. Open Access funding enabled and organized by Projekt DEAL.

Conflict of Interests

The authors declare no conflict of interest.

Keywords: coordination polymer · phosphorus · silver · weakly coordinating anion

[1] a) P. J. Stang, B. Olenyuk, *Acc. Chem. Res.* **1997**, *30*, 502–518; b) M. Fujita, M. Tominaga, A. Hori, B. Therrien, *Acc. Chem. Res.* **2005**, *38*, 369–378; c) M. M. J. Smulders, I. A. Riddell, C. Browne, J. R. Nitschke, *Chem. Soc. Rev.* **2013**, *42*, 1728–1754; d) W. Wang, Y. X. Wang, H. B. Yang, *Chem. Soc. Rev.* **2016**, *45*, 2656–2693; e) C. Lescop, *Acc. Chem. Res.* **2017**, *50*, 885–894; f) W. X. Gao, H. J. Feng, B. B. Guo, Y. Lu, G.-X. Jin, *Chem. Rev.* **2020**, *120*, 6288–6325; g) H.-N. Zhang, X. Huang, G.-X. Jin, *Angew. Chem. Int. Ed.* **2024**, *63*, e202405399; h) W.-L. Shan, H.-H. Hou, N. Si, C.-X. Wang, G. Yuan, X. Gao, G.-X. Jin, *Angew. Chem. Int. Ed.* **2024**, *63*, e202402198.

[2] a) M. J. Zaworotko, *Chem. Commun.* **2001**, 1–9; b) I. Manners, *Angew. Chem. Int. Ed.* **1996**, *35*, 1602–1621; c) S. R. Batten, S. M. Neville, D. R. Turner, *Coordination Polymers: Design*, *Analysis and Application*; Royal Society of Chemistry, **2009**; M.-C. Hong, L. Chen, *Design and Construction of Coordination Polymers*; John Wiley & Sons, **2009**.

[3] a) D. Fujita, Y. Ueda, S. Sato, N. Mizuno, T. Kumasaka, M. Fujita, *Nature* **2016**, *540*, 563–566; b) A. Tarzia, K. E. Jelfs, *Chem. Commun.* **2022**, *58*, 3717–3730; c) T. K. Piskorz, V. Martí-Centelles, T. A. Young, P. J. Lusby, F. Duarte, *ACS Catal.* **2022**, *12*, 5806–5826; d) A. J. McConnell, *Chem. Soc. Rev.* **2022**, *51*, 2957–2971.

[4] W. L. Leong, J. J. Vittal, *Chem. Rev.* **2011**, *111*, 688–764.

[5] a) R. Chakrabarty, P. S. Mukherjee, P. J. Stang, *Chem. Rev.* **2011**, *111*, 6810–6918; b) T. R. Cook, Y.-R. Zheng, P. J. Stang, *Chem. Rev.* **2013**, *113*, 734–777.

[6] a) D. Braga, F. Grepioni, G. R. Desiraju, *Chem. Rev.* **1998**, *98*, 1375–1406; b) S. Leininger, B. Olenyuk, P. J. Stang, *Chem. Rev.* **2000**, *100*, 853–908.

[7] a) O. J. Scherer, *Acc. Chem. Res.* **1999**, *32*, 751–762; b) M. Scheer, *Dalton Trans.* **2008**, *0*, 4372–4386.

[8] a) J. Bai, E. Leiner, M. Scheer, *Angew. Chem. Int. Ed.* **2002**, *41*, 783–786; b) J. Bai, A. V. Virovets, M. Scheer, *Science* **2003**, *300*, 781–783; c) L. J. Gregoriades, J. Bai, M. Sierka, G. Brunklaus, H. Eckert, M. Scheer, *Chem. Eur. J.* **2005**, *11*, 2163–2169; d) E. Peresypkina, C. Heindl, A. V. Virovets, M. Scheer, in *Structure and Bonding, Vol. 174 (*Ed. S. Dehnen), Springer International Publishing, Switzerland, **2016**, pp. 321; e) E. Peresypkina, A. V. Virovets, M. Scheer, *Coord. Chem. Rev.* **2021**, *446*, 213995.

[9] a) M. Scheer, J. Bai, B. P. Johnson, R. Merkle, A. V. Virovets, C. E. Anson, *Eur. J. Inorg. Chem.* **2005**, 4023–4026; b) M. Scheer, A. Schindler, J. Bai, B. P. Johnson, R. Merkle, R. Winter, A. V. Virovets, E. V. Peresypkina, V. A. Blatov, M. Sierka, H. Eckert, *Chem. Eur. J.* **2010**, *16*, 2092–2107; c) M. E. Moussa, M. Fleischmann, E. Peresypkina, L. Dütsch, M. Seidl, G. Balázs, M. Scheer, *Eur. J. Inorg. Chem.* **2017**, 3222–3226; d) P. A. Shelyganov, M. E. Moussa, M. Seidl, M. Scheer, *Angew. Chem. Int. Ed.* **2023**, *62*, e202215650.

[10] M. Scheer, L. J. Gregoriades, A. V. Virovets, W. Kunz, R. Neueder, I. Krossing, *Angew. Chem. Int. Ed.* **2006**, *45*, 5689–5693.

[11] M. Detzel, G. Friedrich, O. J. Scherer, G. Wolmershäuser, *Angew. Chem. Int. Ed.* **1995**, *34*, 1321–1323.

Research Article
doi.org/10.1002/ejic.202400213

[12] a) K. B. Dillon, F. Mathey, J. F. Nixon, in *Phosphorus: The Carbon Copy*; Wiley, New York, **1998**; b) R. Hoffmann, *Angew. Chem. Int. Ed.* **1982**, *21*, 711–724.
[13] J. Bai, A. V. Virovets, M. Scheer, *Angew. Chem. Int. Ed.* **2002**, *41*, 1737–1740.
[14] M. E. Moussa, B. Attenberger, E. V. Peresypkina, M. Scheer, *Dalton Trans.* **2018**, *47*, 1014–1017.
[15] a) E. Peresypkina, K. Grill, B. Hiltl, A. Virovets, W. Kremer, J. Hilgert, W. Tremel, M. Scheer, *Angew. Chem. Int. Ed.* **2021**, *60*, 12132–12142; b) T. Köchner, N. Trapp, T. A. Engesser, A. J. Lehner, C. Röhr, S. Riedel, C. Knapp, H. Scherer, I. Krossing, *Angew. Chem. Int. Ed.* **2011**, *50*, 11253–11256.
[16] The outer diameter of the TEF/FAL anion was calculated as the distance between the two F atoms the furthest apart plus twice the van der Waals radii of F (1.47 Å); A. Bondi, *J. Phys. Chem.* **1964**, *68*, 441–451.
[17] The folding angle is the dihedral angle between either the planes containing P–Ag-P or the plane comprising the central four P atoms and the plane containing P–Ag-P atoms.
[18] R. Blom, T. Brück, O. J. Scherer, *Acta Chem. Scand.* **1989**, *43*, 458–462.
[19] a) O. J. Scherer, T. Brück, *Angew. Chem. Int. Ed.* **1987**, *26*, 59–59; b) M. Baudler, S. Akpapoglou, D. Ouzounis, F. Wasgestian, B. Meinigke, H. Budzikiewicz, H. Münster, *Angew. Chem. Int. Ed.* **1988**, *27*, 280–281.
[20] I. Krossing, *Chem. Eur. J.* **2001**, *7*, 490–502.
[21] CrysAlisPro Software System, Rigaku Oxford Diffraction, (**2018**).
[22] R. C. Clark, J. S. Reid, *Acta Crystallogr.* **1995**, *A51*, 887–897.
[23] O. V. Dolomanov, L. J. Bourhis, R. J. Gildea, J. A. K. Howard, H. Puschmann, *J. Appl. Crystallogr.* **2009**, *42*, 339–341.
[24] G. M. Sheldrick, *Acta Crystallogr.* **2015**, *A71*, 3–8.
[25] G. M. Sheldrick, *Acta Crystallogr.* **2015**, *C27*, 3–8.
[26] M. Scheer, L. J. Gregoriades, A. V. Virovets, W. Kunz, R. Neueder, I. Krossing, *Angew. Chem. Int. Ed.* **2006**, *45*, 5689–5693.
[27] J. Bai, A. V. Virovets, M. Scheer, *Angew. Chem. Int. Ed.* **2002**, *41*, 1737–1740.

Manuscript received: April 15, 2024
Revised manuscript received: April 26, 2024
Accepted manuscript online: April 28, 2024
Version of record online: June 10, 2024